Inorganica Chimica Acta 490 (2019) 235–239

Contents lists available at ScienceDirect

Inorganica Chimica Acta

journal homepage: www.elsevier.com/locate/ica

Structural and biological evaluation of a platinum complex as a potential anti-neurodegenerative agent

Mohammad Azam[a,*], Saikh Mohammad Wabaidur[a], Md. Nazmul Haque[b], Zahid Khan[d], Saud I. Al-Resayes[a], Khalaf A. Al-Foudhily[a], Moon Il Soo[b], Agata Trzesowska-Kruszynska[c], Rafal Kruszynski[c]

[a] Department of Chemistry, College of Science, King Saud University, P. O. Box 2455, Riyadh 11451, Saudi Arabia
[b] Department of Anatomy, Dongguk University Graduate School of Medicine, Gyeongju 38066, Republic of Korea
[c] Institute of General and Ecological Chemistry, Lodz University of Technology, Zeromskiego 116, 90-924 Lodz, Poland
[d] Department of Biochemistry, College of Science, King Saud University, Riyadh, Saudi Arabia

ARTICLE INFO

Keywords:
Platinum complex
Crystal structure
Neuritogenic activity

ABSTRACT

A novel mononuclear platinum complex with N_2O_2 donor atoms was synthesized from the ligand, [N,N′-bis(3-methoxysalicylidene)-2,2-dimethylpropane-1,3-diamine], H2L. The complex was characterized by microanalysis (C, H, N), spectroscopic studies and single crystal X-ray crystallography. The TGA study revealed that the complex degraded in two distinct steps. The effect of the platinum complex was examined by exposing the synthesized complex to rat embryonic hippocampal neurons. The results exhibited significant neuritogenesis at low doses, suggesting it to be a potential therapeutic candidate for combating the neurodegenerative diseases.

1. Introduction

Alzheimer's disease (AD) is the most common form of aging-associated neurodegenerative diseases which is characterized by an irreversible and progressive cognitive dysfunction [1]. Unfortunately, there is no proper therapy for this devastating disease [2,3]. Although the exact cause of AD is not completely known, but the significant evidences suggest that the aggregation of the β-amyloid peptide, a group of 36–42 amino acids, is supposed to be the pivotal and causative factor in the occurrence and development of AD [4–6]. Therefore, aggregation of β-amyloid peptide is the main hallmark for the diagnosis as well as the target for the therapy of this fatal disease. For this purpose, several strategies aiming at diagnosing or treating AD through detection and modulation of Aβ aggregation have been developed, in which the direct interaction with Aβ species has attracted much more attention due to the high efficacy [4,7]. However, neuritogenesis through pharmacological modulation might have potential therapeutic promise in the repairing of damaged neuronal network in degenerating brain disorder like Alzheimer's disease [8]. Over the years, metal ions dyshomeostasis have played significant role in the age-associated neurodegenerative diseases. The free metal ions can bind with the Aβ, since the amyloid β-peptide (Aβ) has metal binding sites with three histidines, and form the metal-peptide complexes to accelerate the peptide aggregation [6,9,10]. The metal-peptide complexes function as seeding factors in the amyloid plaque formation [11], and thus, initiate in the development of diseases as the aggregated Aβ is toxic in nature [12].

Over the past few years, tremendous research efforts were made to design the metal complexes capable of modulating or detecting the Aβ aggregation, necessary for the diagnosis and therapeutics of AD [13–15]. Therefore, Aβ-targeted metal complexes would provide useful strategies for combating AD. The recent investigations by Barnham et al. has shown that the platinum complexes have strong property to weaken the neurotoxicity by inhibiting the aggregation of Aβ [16–18]. Keeping in mind the work of Barnham and his co-workers, we are describing a novel platinum complex derived from ligand, H2L, and exploring its role in the treatment of neurodegenerative disease. The structure of the complex is characterized by single crystal X-ray crystallography, various spectroscopic studies and TGA.

2. Experimental

2.1. Materials and methods

K_2PtCl_4, 2,2-dimethyl-1,3-diaminopropane, o-vanillin, dimethyl sulfoxide and other reagents were purchased from Sigma. The ligand, H2L, and $PtCl_2(DMSO)_2$ were prepared as reported in literature

* Corresponding author.
E-mail address: azam_res@yahoo.com (M. Azam).

https://doi.org/10.1016/j.ica.2019.03.027
Received 3 January 2019; Received in revised form 12 March 2019; Accepted 16 March 2019
Available online 18 March 2019
0020-1693/

[19,20]. The complex was investigated by carbon, hydrogen and nitrogen analyses, FT-IR and NMR spectroscopic studies using Elementar Varrio EL analyzer, Perkin Elmer 621 spectrophotometer and JEOL spectrometer at 400 MHz in d_6-DMSO, respectively. The TGA was reported in nitrogen at heating rate 20 °C/minute using Mettler Toldo Switzerland, TGA1/DSC instrument. The Mass spectrometry of the platinum complex was performed with the aid of Micromass Quattro Premier tandem mass spectrometer.

2.2. Synthesis of platinum complex

An alcoholic solution of ligand, H2L (100 mg, 0.27 mmol) was mixed with $[PtCl_2(DMSO)_2]$ in 1:1 equimolar ratio, and magnetically stirred for 10 h at room temperature, leading to the formation of an orange coloured solution with slight turbidity. The coloured crystals were obtained within a week at room temperature after removing the turbidity.

Yield: 65%; Colour: orange; Analytical calculation for $C_{21}H_{24}N_2O_4Pt$: (Calculated): C, 44.76; H, 4.29; N, 4.97; (Found): C, 44.71; H, 4.25; N, 4.95; ^{1}H NMR (d_6-DMSO) δ (ppm) 8.49 (s, 2H), 6.37–7.22 (6H, m); IR (cm^{-1}): 1610 (s)

2.3. Crystal structure measurement

The crystallographic data were collected using Rigaku Synergy Dualflex automatic diffractometer equipped with Pilatus 300 K detector, and monochromated MoK_α (λ = 0.71073 Å) radiation at room temperature. The structure was solved using the SHELXS [21], SHELXL [22] and SHELXTL [23] programs. The refinement details, selected bond length and angles are provided in Tables 1–3, respectively. The atomic scattering factors were taken from the literature [24]. [For detailed crystal measurement, please see Supplementary information].

2.4. Cell culture and drug treatment

All the experiments were accomplished using the protocols approved by the Dongguk University Animal Care and Use Committee (approval certificate number IACUC-2015-002). Embryonic day 19 (E19) pups brain from Sprague–Dawley rat strain were used to prepare primary hippocampal neurons. Briefly, fetal hippocampi obtained from the isoflurane anesthetized pregnant rat were dissociated and neuronal cultures were prepared as defined earlier [25]. Cells were grown in serum-free neurobasal medium supplemented with B-27 at 37 °C in a humidified 5% CO_2 incubator. Platinum complex or vehicle [DMSO, final concentration < 1.0% (v/v)] were added to the growth media before cell plating. Unless otherwise specified, all cell culture reagents were purchased from Invitrogen (Carlsbad, CA).

Table 1
Crystal and structure refinement data of Pt compound.

Empirical formula	$C_{21}H_{26}N_2O_5Pt$
Formula weight	581.53
Crystal system, space group	monoclinic, $P2_1/n$ (No.14)
Unit cell dimensions [Å, °]	a = 13.7159(2) b = 10.3204(2) c = 14.9899(3) β = 104.595(2)
Volume [Å^3]	2053.40(7)
Z, Calculated density [Mg/m^3]	4, 1.881
F(0 0 0)	1136
Crystal size [mm]	0.127, 0.114, 0.099
θ range for data collection [°]	3.433 to 32.272
Index ranges	$-20 \le h \le 19$, $-13 \le k \le 13$, $-20 \le l \le 22$
Reflections collected/unique	42254/6404 [$R_{(int)}$ = 0.0828]
Completeness [%]	99.8 (to θ = 25°)
Data/restraints/parameters	6404/0/266
Goodness-of-fit on F^2	1.033
Final R indices [$I > 2\sigma(I)$]	$R1$ = 0.0436, $wR2$ = 0.1086
R indices (all data)	$R1$ = 0.0571, $wR2$ = 0.1186
Largest diff. peak and hole [e·Å^{-3}]	3.727 and −4.438

Table 2
Selected structural data of Pt compound [Å, °].

Pt1–N2	1.979(4)
Pt1–N1	2.005(4)
Pt1–O1	2.016(4)
Pt1–O2	2.021(3)
C7–N1	1.292(6)
N1–C8	1.489(6)
C10–N2	1.486(6)
N2–C11	1.292(6)
N2–Pt1–N1	94.67(17)
N2–Pt1–O1	172.50(15)
N1–Pt1–O1	92.79(15)
N2–Pt1–O2	92.26(15)
N1–Pt1–O2	172.77(14)
O1–Pt1–O2	80.31(14)

Table 3
Hydrogen bonds geometry of Pt compound [Å, °].

D–H···A	d(D-H)	d(H···A)	d(D···A)	< (DHA)
O5–H5O···O2	0.84	2.56	3.350(5)	156.5
O5–H5P···O3	0.90	1.90	2.772(6)	164.0
O5–H5O···O4	0.84	2.06	2.720(6)	135.7
C5–H5···O5^{i}	0.93	2.52	3.431(7)	166.2
C8–H8B···O4^{ii}	0.97	2.54	3.498(6)	169.3
C10–H10A···O1^{ii}	0.97	2.65	3.330(7)	127.5
C21–H21C···O2^{iii}	0.96	2.57	3.429(7)	148.5

Symmetry transformations used to generate equivalent atoms: (i) x − 1/2, −y + 1/2, +z − 1/2; (ii) −x + 1, −y + 1, −z + 1; (iii) −x + 3/2, y + 1/2, −z + 3/2.

2.5. Immunofluorescence microscopy

Neuronal cells were fixed sequentially with 4% paraformaldehyde in phosphate-buffered saline at room temperature for 10 min followed by methanol at −20 °C for 20 min [26]. Cells were treated with neuron specific mouse monoclonal microtubule-associated protein 2 antibody (MAP2; 1:500). Specific binding of primary antibody was visualized by Alexa fluor 488-conjugated goat anti-mouse IgG secondary antibody [1:1000, Molecular Probes, Eugene, OR]. Stained cells were visualized under Leica DM IRE2 microscope. Images were captured with high-resolution CCD camera (CoolSNAPTM; Photometrics Inc., Tucson, AZ) and Leica FW4000 program and further processed using Adobe Photoshop 7.0. A minimum of 30 cells were examined for morphometric analysis as described previously [25]. Image J software (version 1.45) plug-in with simple neurite tracer (National Institute of Health, Bethesda, MD) was used for this analysis.

2.6. Statistical analysis

Three independent experiments were conducted and outcomes are provided as the means ± SEM. For statistical analyses, we used ANOVA in SPSS version 17.0 (SPSS Inc.). P values < 0.05 were supposed to be statistically significant.

3. Results and discussion

The molecular structure of platinum complex is given in Fig. 1, which consists of complex molecules derived from the doubly deprotonated N,N′-2,2′-dimethylpropylenebis (3-methoxysalicylideneiminato) ligand chelating with the Pt^{2+} cation and the water molecule located outside the coordination sphere. The complex molecule

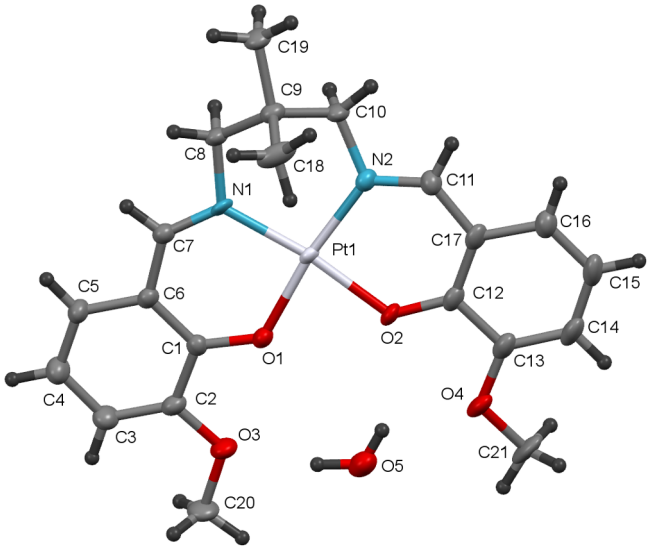

Fig. 1. The molecular structure of platinum complex.

possesses the pseudo symmetry mirror plane going through the Pt1, C9, C18 and C19 atoms. Consequently, the respect pairs of analogous atoms of studied compound are related by non-crystallographic, above mentioned, pseudosymmetry element. This structural effect is distinctly different than observed in other coordination compounds of this ligand [27–30], in which the pseudosymmetry two-fold rotation axis exists. The platinum atom adopts formally ideal quadrilateral planar geometry with sum of interbond angles centred at metal atom equal to 360.0°. The difference between ideal (90°) and observed (Table 2) angles between coordination bond vary from 2° to 10°, what indicated considerable distortion from square planar coordination geometry. This distortion is caused by the relatively rigid geometry of chelating ligand and consequently imposed restrains of coordination geometry. The salicylidene-1-methaneaminato moieties are almost planar, similarly to the conformation of comparable ligand [31] and its copper coordination compound [32–34].

The complex and solvent molecules of the platinum complex are assembled to supramolecule by three O—H···O hydrogen bonds, of which two form three-cantered interaction based on bifurcated donor (Table 3). Those interactions form finite patterns (designator: D [35]) of unitary graph set of lowest degree, and $R_1^2(5)$, $R_2^2(9)$, $R_2^2(12)$ ring patterns of binary graph set. The crystal net is stabilised by additional four structurally different week C—H···O hydrogen bonds [36], which assemble of complex and solvent molecules to the two dimensional layer extending along crystallographic (1 0 −1) plane. This layer is additionally interlinked by π···π staking interactions between neighbouring complex molecules (Table 4) [37].

The characteristic IR absorption band due to azomethine vibration appeared at 1610 cm^{-1} [38]. Appearance of a broad band at 3375 cm^{-1} is reasonably assigned to water lying in the complex [39–41]. Furthermore, absorption bands due to —C—O, C═C, and C—H groups are found at 1180 cm^{-1}, 1459 cm^{-1} and 2969 cm^{-1} respectively [Fig. S1] [39–41].

The characteristic resonance due to azomethine proton appeared at 8.49 ppm in the ^{1}H NMR spectrum of the platinum complex. However, the signals assigned to $-CH_2$ and $-O-CH_3$ protons appeared at 3.10 ppm and 3.76 ppm, respectively, whereas the signals at 6.37–7.22 ppm were assigned to aromatic ring protons. The resonating signals corresponding to $-CH_3$ protons displayed at 1.18 ppm.

Mass spectrum of the platinum complex exhibited a molecular ion peak (m + 1) *m/z* at 582.5, which is corresponding to its molecular weight, and equivalent to the corresponding structure shown in Fig. 1 [Fig S2].

The thermogravimetric analysis was investigated in inert environment of nitrogen at temperature 0–800 °C. The complex degraded in two steps with the loss of water molecule (3.09%) lying in the lattice of crystal structure in the initial step of degradation at temperature upto 200 °C. However, upon increasing the temperature, there was rapid weight loss of ca. 36.11% at 250–330 °C, suggesting the complete degradation of organic moiety in the complex. On further heating, horizontal line was shown in the thermogram, indicating the formation of metal oxide as final decomposition product [Fig. S3].

3.1. Neuritogenic promoting activity of the platinum complex on rat E19 hippocampal cells

Cultured E19 rat hippocampal neurons were utilized to examine the neurotrophic factor-mimetic property of the synthesized compound. Neuronal cells were treated with DMSO (vehicle) and increasing concentrations of the complex for three days, and morphometric parameters were analysed as described earlier [25]. Quantitative immunofluorescent analysis revealed that the platinum complex promotes neuritogenic effect on hippocampal neurons. Interestingly, we observed statistically significant increase in PNN by ~36% ($P < 0.05$), ~50% ($P < 0.001$) (Fig. 2B-a); TLPN by ~99% ($P < 0.001$), ~94% ($P < 0.001$) (Fig. 2B-b); LLPN by ~165% ($P < 0.001$), ~140% ($P < 0.001$) (Fig. 2B-c) relative to vehicle at concentration of 4.5 μM and 13 μM, respectively. There was no significant neuritogenesis stimulation at 26 μM for any of the analysed morphometric parameters, whereas the higher concentration of the complex at 5.4 μM resulted in acute toxicity observed by the death of hippocampal neuronal culture.

Neuronal development involves extremely organized processes comprising neurite outgrowth, axonal growth, dendritic growth and branching, and ultimately leading to maturation by forming synapses through dendritic spines. Neuritogenesis requires a complex interplay of intracellular and extracellular signals where the neurotrophic factors play the central role [42,43]. The resulting neurites form the structural and functional polarity as well as synaptic connections during development by establishing highly interconnected neuronal networks in the brain [44–46]. Neurodegenerative diseases are characterized by severe atrophy of the neuronal cells. Under such conditions, neurotrophic compounds of natural or synthetic origin which stimulate neurite development could be useful for the treatment of neurological disorders [47]. Hence, the main focus of this research is to investigate the neurotrophic potential of the platinum complex possessing H2L regarding the neuritogenic activity which may help in repairing the damage in degenerating brain through support neuronal networks by inducing axonal sprouting and dendritic remodelling [8,48]. Our results from the treatment of rat embryonic hippocampal cells showed that the platinum complex has potential neuritogenic activity as observed by modification of neuronal cytoarchitecture and neuronal sprouting which may promote neuronal networks in the brain. Further investigations regarding the elucidation of underlying mechanism of action as well as to evaluate minimum uptake of the studied platinum complex by the cell, which is sufficient for its neurotrophic activity, are required either through *in vitro* or in vivo analysis

Table 4
Stacking interactions in Pt compound [Å, °]. Cg(1), Cg(2), Cg(3) indicates the centroids of six-membered pyridine rings (R) containing C1 and C11 atoms respectively, α is a dihedral angle between planes I and J, β is an angle between Cg(I)-Cg(J) vector and normal to plane I and d_p is a perpendicular distance of Cg(I) on ring J plane.

R(I)···R(J)	Cg···Cg	α	β	d_p
Cg(1)···Cg(2)^{iv}	4.543(3)	2.4(3)	41.0	3.307(2)
Cg(2)···Cg(1)^{iv}	4.543(3)	2.4(3)	43.3	3.428(2)

Symmetry transformations used to generate rings: (iv) −x + 1, −y + 1, −z + 1.

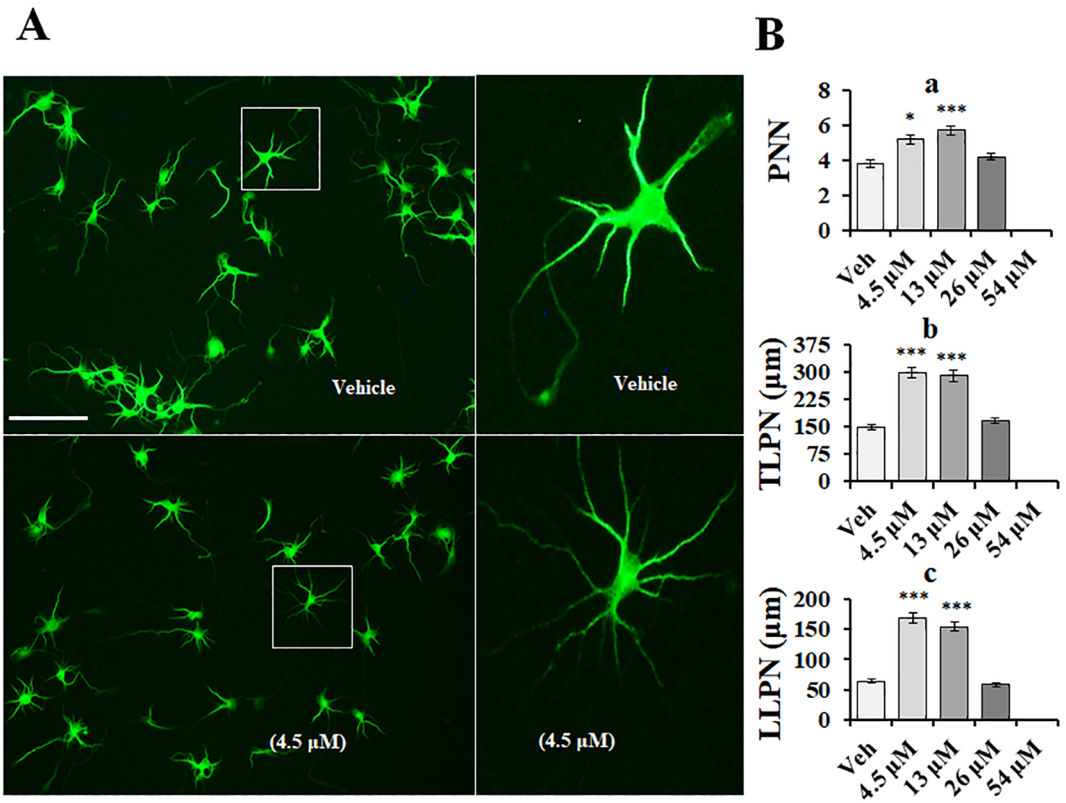

Fig. 2. Evaluation of the neuritogenic activities of the platinum complex. The complex was added to hippocampal cultures at different concentrations for 3 days. Result represents representative fluorescence photomicrograph after treatment of different compound with their highest neuritogenic activity (Fig. 2A). The statistical analysis differential neuritogenic activity of different compound at various concentrations were conducted to determine the effects primary hippocampal neurons on the basis of various morphometric characters that is (Fig. 2B-a) the primary neurites number (PNN, neurites originated directly from soma), (Fig. 2B-b) total length of primary neurites (TLPN; sum of the length of primary neurites) and (Fig-2B-c) the longest length of primary neurites (LLPN). Scale bar 40 µm. Bars represent means ± SEM (n = 30 individual neurons). Statistically significant vs. vehicle: $^{*}p < 0.05$, $^{**}p < 0.01$, and $^{***}p < 0.001$ (ANOVA).

4. Conclusion

We have successfully synthesized a novel platinum complex possessing N_2O_2 donor atoms and its usage as a potential anti-neurodegenerative agent.

Acknowledgments

The authors would like to extend their sincere appreciation to the Deanship of Scientific Research at king Saud University for funding this work through research group project number RG-1436-003.

Appendix A. Supplementary data

The whole crystallographic data has been deposited with the Cambridge Crystallographic Data Centre under No. CCDC 1866259. Supplementary data to this article can be found online at https://doi.org/10.1016/j.ica.2019.03.027.

References

[1] L. Mucke, Nature 461 (2009) 895–897.
[2] K.P. Kepp, Chem. Rev. 112 (2012) 5193–5239.
[3] D.J. Selkoe, Science 337 (2012) 1488–1492.
[4] R. Jakob-Roetne, H. Jacobsen, Angew. Chem. Int. Ed. 48 (2009) 3030–3059.
[5] L. Larbanoix, C. Burtea, E. Ansciaux, S. Laurent, I. Mahieu, E.L. Vander, R.N. Muller, Peptides 32 (2011) 1232–1243.
[6] M. Ahmed, J. Davis, D. Aucoin, T. Sato, S. Ahuja, S. Aimoto, J.I. Elliott, W.E.V. Nostrand, S.O. Smith, Nat. Struct. Mol. Biol. 17 (2010) 561–567.
[7] K. Blennow, Nat. Med. 16 (2010) 1218–1222.
[8] B. Teter, J.W. Ashford, J. Neurosci. Res. 70 (2002) 402–437.
[9] S.C. Drew, C.L. Masters, K.J. Barnham, J. Am. Chem. Soc. 131 (2009) 8760–8761.
[10] S.C. Drew, C.J. Noble, C.L. Masters, G.R. Hanson, K.J. Barnham, J. Am. Chem. Soc. 131 (2009) 1195–1207.
[11] V. Chauhan, L. Ji, A. Chauhan, Biogerontology 9 (2008) 381–389.
[12] J. Hardy, D.J. Selkoe, Science 297 (2002) 353–356.
[13] V.B. Kenche, L.W. Hung, K. Perez, Angew. Chem. Int. Ed. 52 (2013) 3374–3378.
[14] F. Collin, I. Sasaki, H. Eury, P. Faller, C. Hureau, Chem. Commun. 49 (2013) 2130–2132.
[15] S. Lim, B.M. Paterson, M.T. Fodero-Tavoletti, Chem. Commun. 46 (2010) 5437–5439.
[16] V.B. Kenche, L.W. Hung, K. Perez, I. Volitakes, G. Ciccotosto, J. Kwok, N. Critch, N. Sherratt, M. Cortes, V. Lal, C.L. Masters, K. Murakami, R. Cappai, P.A. Adlard, K.J. Barnham, Angew. Chem. 125 (2013) 3458–3462.
[17] V.A. Streltsov, V.C. Epa, S.A. James, Q.I. Churches, J.M. Caine, V.B. Kenche, K.J. Barnham, Chem. Commun. 49 (2013) 11364–11366.
[18] G.S. Yellol, J.G. Yellol, V.B. Kenche, X.M. Liu, K.J. Barnham, A. Donaire, C. Janiak, J. Ruiz, Inorg Chem. 54 (2015) 470–475.
[19] A. Bhattacharyya, S. Roy, J. Chakraborty, S. Chattopadhyay, Polyhedron 112 (2016) 109–117.
[20] J.H. Price, A.N. Williamson, R.F. Schramm, B.B. Wayland, Inorg. Chem. 11 (1972) 1280–1284.
[21] G.M. Sheldrick, Acta Crystallogr., Sect. A 71 (2015) 3–8.
[22] G.M. Sheldrick, Acta Crystallogr., Sect.C 71 (2008) 3–8.
[23] G.M. Sheldrick, Acta Crystallogr., Sect.A 64 (2008) 112–122.
[24] E. Prince (Ed.), International Tables for Crystallography, Volume C: Mathematical, Physical and Chemical Tables, 3rd ed., Kluwer Academic Publishers, Dordrecht, 2004.
[25] M.A. Hannan, J.Y. Kang, Y.K. Hong, Phytother. Res. 27 (2013) 21–29.
[26] I.S. Moon, S.J. Cho, I. Jin, R. Walikonis, Mol. Cells 24 (2007) 76–82.
[27] J.-P. Costes, B. Donnadieu, R. Gheorghe, G. Novitchi, J.-P. Tuchagues, L. Vendier, Eur. J. Inorg. Chem. (2008) 5235–5244.
[28] C.S. Yeap, R. Kia, H. Kargar, H.-K. Fun, Acta Crystallogr. Sect. E: Struct. Rep. Online 65 (2009) m570–m571.
[29] H.-H. Yao, W.-T. Huang, J.-M. Lo, F.-L. Liao, P. Chattopadhyay, J. Coord. Chem. 58 (2005) 975–984.
[30] S. Rayati, S. Zakavi, M. Koliaei, A. Wojtczak, A. Kozakiewicz, Inorg. Chem. Commun. 13 (2010) 203–207.
[31] P. Corden, W. Errington, P. Moore, M.G.H. Wallbridge, Acta Crystallogr., Sect. C: Cryst. Struct. Commun. 52 (1996) 125–127.
[32] B.H. Chen, H.H. Yao, W.T. Huang, P. Chattopadhyay, J.M. Lo, T.H. Lu, Solid State

Sci. 1 (1999) 119–131.
[33] C. Arici, F. Ercan, R. Kurtaran, O. Atakol, Acta Crystallogr., Sect. C: Cryst. Struct. Commun. 57 (2001) 812–814.
[34] M. Azam, S. Dwivedi, S.I. Al-Resayes, S.F. Adil, M.S. Islam, A. Trzesowska-Kruszynska, R. Kruszynski, D.-U. Lee, J. Mol. Struct. 1130 (2017) 122–127.
[35] J. Bernstein, R.E. Davis, L. Shimoni, N.-L. Chang, Angew. Chem. Int. Ed. Engl. 34 (1995) 1555–1573.
[36] G.R. Desiraju, T. Steiner, The Weak Hydrogen Bond in Structural Chemistry and Biology, Oxford University Press, Oxford, 1999.
[37] R. Kruszynski, T. Sieranski, Cryst. Growth Des. 16 (2016) 587–595.
[38] M. Azam, S.I. Al-Resayes, S.M. Soliman, A. Trzesowska-Kruszynska, R. Kruszynski, Z. Khan, J. Photochem. Photobiol. B: Biol. 176 (2017) 150–156.
[39] R.S. Drago, Physical Methods in Inorganic Chemistry, East-West Press Pvt. Ltd., New Delhi, 1968.
[40] K. Nakamoto, Infrared and Raman Spectra of Inorganic and Coordination Compounds, Wiley, New York, 1986.
[41] N.S. Abdel-Kadera, A.L. El-Ansarya, T.A. El-Tayebb, M.M.F. Elnagdi, J. Photochem. Photobiol. A: Chem. 321 (2016) 223–237.
[42] J.L. Goldberg, J.S. Espinosa, Y. Xu, N. Davidson, G.T. Kovacs, B.A. Barres, Neuron 33 (2002) 689–702.
[43] S.I. Lentz, C.M. Knudson, S.J. Korsmeyer, W.D. Snider, J. Neurosci. 19 (1999) 1038–1048.
[44] C.G. Dotti, C.A. Sullivan, G.A. Banker, J. Neurosci. 8 (1988) 1454–1468.
[45] E.F. Fornasiero, D. Bonanomi, F. Benfenati, F. Valtorta, Cell Mol. Life Sci. 67 (2010) 1383–1396.
[46] E. Bullmore, O. Sporns, Nat. Rev. Neurosci. 13 (2012) 336–349.
[47] N. Kaneko, K. Sawamoto, Neurosci. Res. 63 (2009) 155–164.
[48] A.K. McAllister, Cereb. Cortex 10 (2000) 963–973.